Numerical parametric study on corrugated web built-up beams with pinned end supports

Lukačević, Ivan; Ungureanu, Viorel

CFSRC COLLOQUIUM

Proceedings of the Cold-Formed Steel Research Consortium Colloquium
17-19 October 2022 (cfsrc.org)

Numerical parametric study on corrugated web built-up beams with pinned end supports

Ivan Lukačević[1], Viorel Ungureanu[2]

Abstract

Cold-formed steel elements are commonly used in construction due to their advantages, such as material savings and reduced self-weight. Such advantages can be significantly enlarged by using built-up solutions. Such solutions have been presented in the literature over the past few decades. The most common way to assemble such elements are using screws or bolts. However, the developments in the welding processes also lead to other solutions, such as continuous (laser or MIG brazing) or discrete (spot welding). Corrugated web beams are one of these built-up solutions. On the basis of previous experimental and numerical studies on such built-up beams, it was concluded that the capacity of the cold-formed steel built-up steel beams with the corrugated web with fixed end supports is highly affected by the type of connections and the geometry of the system and components, especially its corrugated web and shear panels near supports. To find the optimal geometry of such beams with nominally pinned end supports, the paper starts by summarising the previous experimental investigations on cold-formed steel built-up corrugated web beams and, based on a calibrated numerical model, presents the parametric numerical investigation of such beams with different configurations. The influence of several parameters has been investigated, i.e. the influence of different end supports conditions for beams with single and double web, the influence of the number of spot welds on flanges, the influence of changing from discrete to continuous connections between beam components, the influence of the distance between spot welds on flanges, influence of the flange's thickness, the influence of corrugated web thickness and the influence of the shear panel thickness. The parametric study shows that changing end support conditions can significantly reduce the complexity of the analysed beam support and its cost without a significant decrease in beam performances related to its rigidity and bending capacity. The new solution presented of corrugated web beams with double corrugated web shows a significant contribution in flexural rigidity and bending capacity. Changing the type of connection between beam elements from discrete spot welding to continuous connection results in a higher capacity and rigidity of these beams. On the other hand, increasing the number of spot welds from 2 to 3 per corrugation between the web and the flanges can have a certain influence on the increase of the ultimate bending capacity while initial flexural stiffness remains almost the same. The distance between the spot welds on the flanges shows a very small influence on the behavior of the beam. Increasing the thicknesses of the beam elements can significantly increase the flexural stiffness and bending capacity of the beam, and the optimal beam configuration will be investigated in future studies.

1. Introduction

The research in this paper is related to a new technological solution for the built-up beams made of corrugated steel sheets for the web and thin-walled cold-formed steel profiles for the flanges, connected by resistance spot welding (SW), i.e. CWB beams [1–3]. Within the parametric numerical study with the finite element (FE) software Abaqus/CAE [4], the investigation focuses on the possibility and effectiveness of double corrugated web and nominally pinned end supports.

The numerical models were calibrated and validated based on experimental tests of similar elements carried out within the WELLFORMED research project at the CEMSIG Research Center of the Politehnica University of Timisoara. The mechanical properties of the base material and the test results of two built-up corrugated web beams (CWB) were presented in detail by Ungureanu et al. [1]. A 500 kN actuator loaded the beam through a leverage system that evenly distributes the load in 4 points to simulate a uniform distributed load in a planar rigid frame with both ends fixed to the frame, as shown in Figure 1. The deformed shape of the numerical model, presented in Figure 1, exhibits the phenomena encountered during the experiments, such as shear panel buckling, distortion of the corrugated web and the local buckling of the flange in the load application points.

[1] Assistant Professor, Structural Engineering Department, Faculty of Civil Engineering, University of Zagreb, ivan.lukacevic@grad.unizg.hr
[2] Full Professor, Steel Structures and Structural Mechanics Department, Politehnica University of Timisoara, viorel.ungurenu@upt.ro

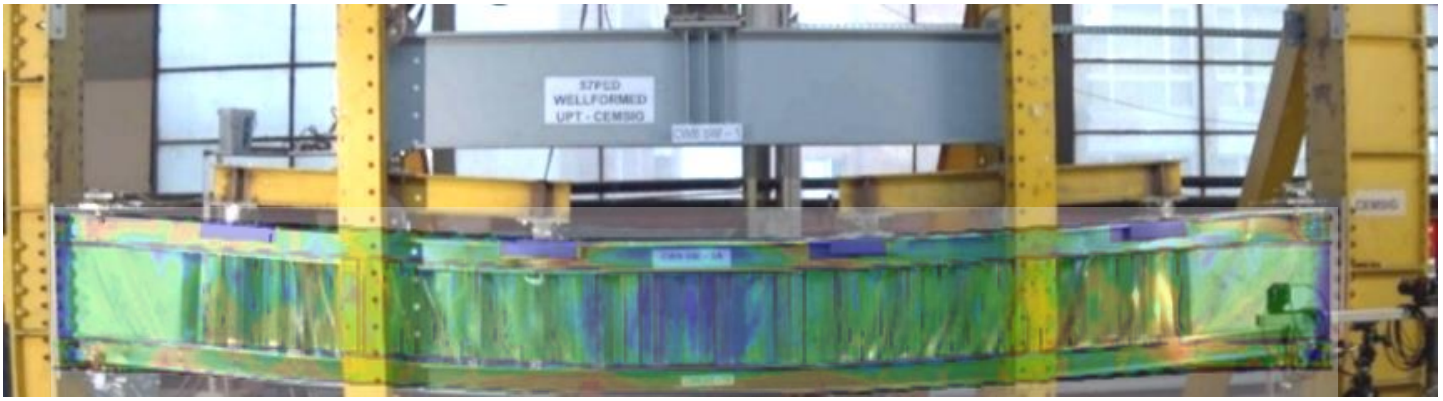

Figure 1: Tested beam CWB SW-1 and results of calibrated FE model over it [5,6]

The specimens of built-up CWB have a span of 5157 mm, a beam height of 600 mm, and a corrugation height of 60 mm.

The beams consisted of the following components: corrugated steel sheet for the web - 0.8 mm (mid-span) and 1.2 mm (beam ends); additional shear panels - flat plates of 1.0 mm (CWB SW-1) and of 1.2 mm (CWB SW-2); two back-to-back lipped channel sections for flanges - 2 × C120x47x2.0; reinforcing profiles U150x70x2.0 used under the load application points; bolts M12 grade 8.8 for the flange to end plates connections. For CWB specimens, the 1.0 mm sheet for the corrugated web is classified as S250GD+Z, while the 1.2 mm and the 2.0 mm thicknesses for the shear panels and for the flanges, respectively, have a steel grade S350GD+Z steel.

The tested beams CWB SW-1 and CWB SW-2 have different thicknesses for the shear panels and a different configuration of the spot welding fastenings used to connect the corrugated web panels, as presented in [1]. The same number of spot welding (SW) was used to connect the corrugated sheets, i.e. for the CWB SW-1 beam, the connections were made in two rows on the incline webs, while for the CWB SW-2 beam, the corrugated sheets were connected in one row only on the rest of the corrugated sheet [1].

Figure 2 compares the experimental load-displacement curves for the CWB SW-1 beam, whereas Figure 3 compares the experimental load-displacement curves for the CWB SW-2 beam from the papers [5,6].

In order to find the optimal geometry of such beams with nominally pinned end supports, the paper presents the results of the parametric numerical investigation. The influence of several parameters has been investigated, i.e. influence of different end supports condition for beams with single and double web, the influence of the number of spot welds on flanges, the influence of changing from discrete to continuous TIE connections between beam elements, the influence of the distance between spot welds on flanges, influence of the flange's thickness, influence of corrugated web thickness and influence of the shear panel thickness.

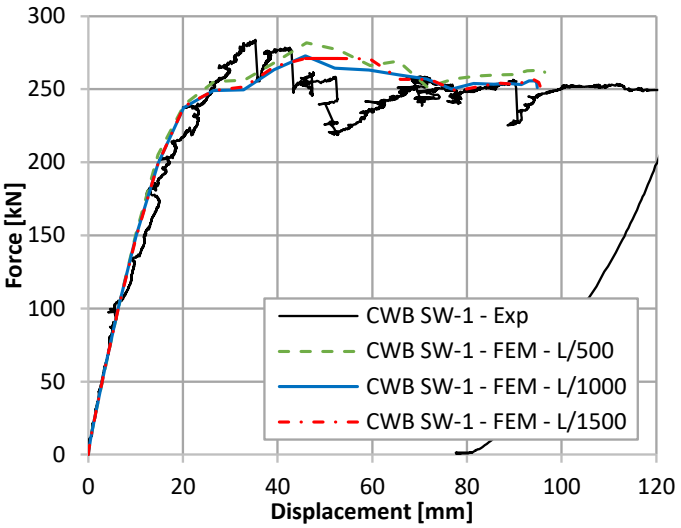

Figure 2: Experimental vs. FEM load-displacement curves for the CWB SW-1 beam [5,6]

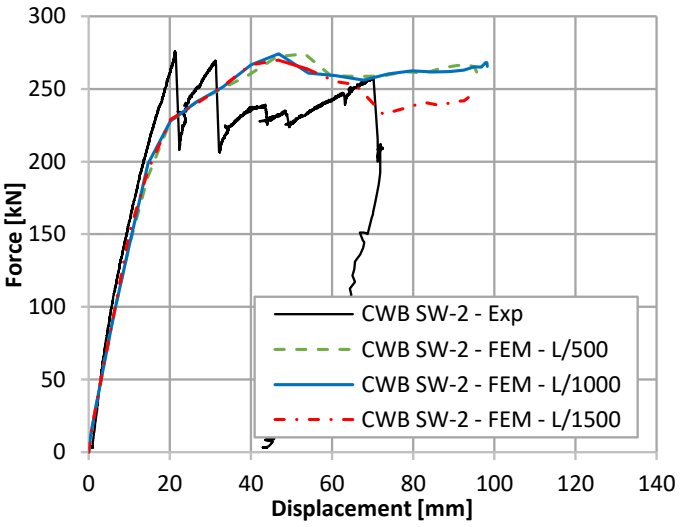

Figure 3: Experimental vs. FEM load-displacement curves for the CWB SW-2 beam [5,6]

2. Preparation of the numerical model

The general-purpose finite element program ABAQUS/CAE v.6.14 [4] was used to perform nonlinear geometric and material analyses, including the effects of initial imperfections (GMNIA). FE models have been calibrated in accordance with the experimental results of input parameters such as experimentally measured properties of materials and tensile-shear tests on the lap joint welded specimens. Initial geometric imperfections, mesh size, and element type have been calibrated following the experimental results of tested beams as presented in papers [5,6]. Each part of the built-up beam has been defined as a 3D shell element extruded according to the shape of the part. Rectangular 4-node doubly curved thin or thick shell, reduced integration, hourglass control, and finite membrane strains (S4R) were used to model the thin-walled components. The global mesh size of 15 mm was used for the web, flanges, and shear panels, and 25 mm for the reinforcing profiles according to the load application [3]. The mesh size was further reduced around the bolt holes that connect the shear panels to the end plates.

General contact was used with the following parameters between all elements of the model, that is, normal direction - hard contact, transverse direction - a friction coefficient of $\mu = 0.1$ and separation was allowed after the general contact took place.

The models with a single and double corrugated web with parts are presented in Figure 4.

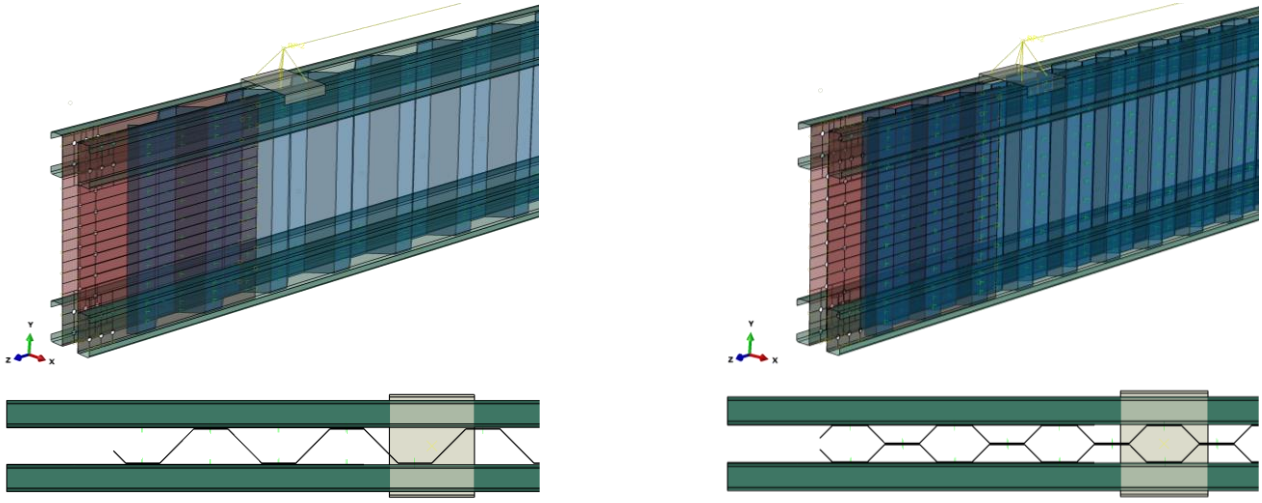

a) calibrated FE model of CWB b) FE model of double CWB

Figure 4: Parts of the CWB FE models by components: green (flanges), red (shear panels), blue (web)

Previous studies, considering appropriate imperfections, material parameters, mesh size and element type, have shown that FE models can be used to accurately predict the load carrying capacity and post-buckling behaviour of the built-up cold-formed steel beams [2,5-7].

While the support conditions were defined on the nodes of the holes provided for the bolts that connect the beam to the end plate assembly as null displacements and rotations, the loading of the beam was defined as a vertical displacement in a set of multipoint constraints MPC that forms a leverage system to transmit the deflection to the four loading points (see Figure 5). The link between the control points and the pressure surface was defined by a kinematic coupling constraint for all DOFs. The RB3D2 elements were used as a rigid body for load transfer and the multipoint constraint beam (MPC beam) for DOF coupling between groups of specified nodes.

The spot welds (SW) between different parts of the built-up beams were defined as functions of the tensile-shear tests of the simple specimens as follows. Attachment points were defined in each part where SW was applied. The connection between the attachment points was defined using Point Based Fasteners with the Connector response of the SW initially calibrated from the tensile-shear test results. The connector was considered by the elasticity, plasticity, damage, and failure parameters. Bushing connector elements were used to model the SW. This type of element provides a connection between two nodes that allows independent behaviour in three local Cartesian directions that follow the system at both nodes and that allows different behaviour in two flexural rotations and one torsional rotation [4].

In order to obtain realistic results from the non-linear finite element analyses, plastic strains were included in the material definition, according to EN1993-1-5, Annex C [8].

The measured stress-strain curves based on tensile tests on coupons cut from the cross-section of component elements were included in the model. In the plastic analysis, the static engineering stress-strain curves obtained from tensile coupon tests were converted to true stress vs logarithmic true plastic strain curves. The true stress σ_{true} and true plastic strain ε_{true} were calculated using equations (1) and (2) as follows:

$$\sigma_{\text{true}} = \sigma_{\text{engineering}}\left(1 + \varepsilon_{\text{engineering}}\right) \quad (1)$$

$$\varepsilon_{\text{true}} = ln\left(1 + \varepsilon_{\text{engineering}}\right) \quad (2)$$

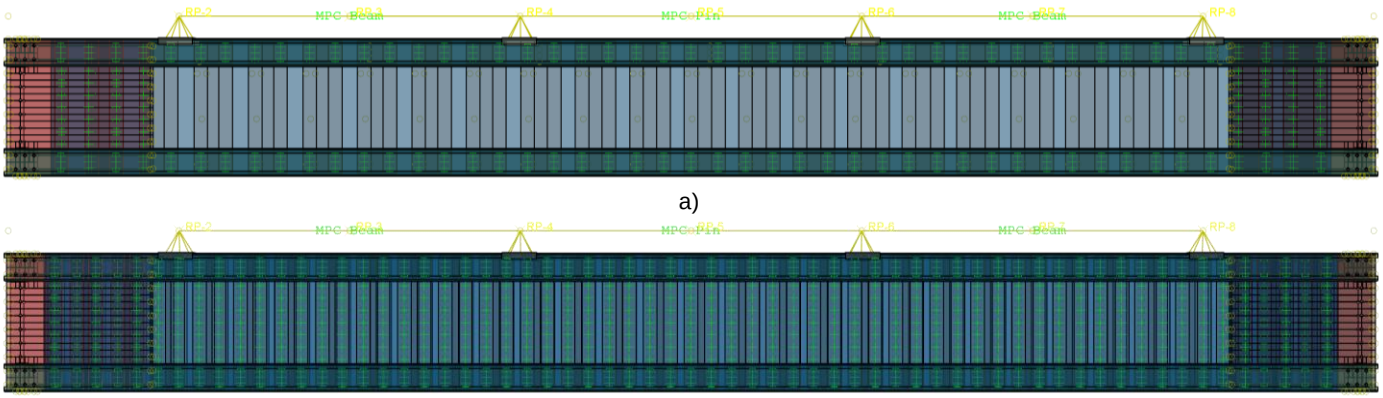

a)

b)

Figure 5: Load introduction in FE models: a) calibrated FE model of CWB, b) FE model of double CWB

In order to include plasticity within ABAQUS, the stress-strain points past yield must be input in the form of true stress and logarithmic plastic strain. The logarithmic plastic strain has been calculated with equation (3) as follows:

$$\varepsilon_{\text{ln}}^{\text{plastic}} = \varepsilon_{\text{true}} - \frac{\sigma_{\text{true}}}{E} \quad (3)$$

where σ_{true}/E is the elastic strain and E is Young's modulus. The numerical model consists of two steps. In the first step, the initial imperfections are modelled by performing static non-linear analysis with the target displacements, which results in desired imperfection. In the second step, the dynamic, explicit analysis is used to run the load-displacement analysis of the beam based on geometry from previous static analysis for imperfections and with all contacts and material nonlinearity included.

For the parametric study in this paper, the model with an initial out of global web imperfections with magnitudes of approximately L/1000 and cross-sectional imperfections (local and distortional) with a magnitude of approximately equal to the thickness of the sheet *t* has been adopted [5,6].

3. Parametric numerical study

A parametric numerical study was used to investigate the influence of the following parameters: influence of different end supports condition for beams with single and double web, the influence of the number of spot welds on flanges, influence of changing from discrete to continuous TIE connections between beam elements, the influence of the distance between spot welds on flanges, influence of the flange's thickness, the influence of corrugated web thickness and influence of the shear panel thickness.

For the following model references to the results, the name represents the characteristics of the model. An example 6_M_C120_25_EXP_DW_pin stands for: 6_M = 6 m span, C120 = the channel section, 25 = flange profile thickness 2.5 mm (10 = 1.0 mm, 12 = 1.2 mm, 15 = 1.5 mm, 20 = 2.0 mm), DW = double web (without the DW = single web), pin = nominally pinned supports (without the word pin = fixed supports). Other notations are: 3SW = 3 spot welds (without the 3SW = 2 spot welds), DIST = increased vertical distance between SW, TIE = all elements are connected with tie connection without SW, SP00 = the shear panel thickness of 0.0 mm (without the SP = 0.8 mm, SP10 = 1.0 mm, SP12 = 1.2 mm, SP15 = 1.5 mm), W10 = the corrugated web thickness of 1.0 mm (without the W = 0.8 mm, W12 = 1.2 mm, W15 = 1.5 mm). All models were analysed with a constant height of 600 mm.

3.1 Influence of different end supports condition

The calibrated model presented in the papers [5,6] has been extended to a length of 6 m, and the influence of different end support conditions was investigated. Both solutions of CWB with single and double web are considered with different end supports presented in Figure 6. Figures 6 a) and b) present the fixed and nominally pinned support (only the upper flange of CWB is fixed) for CWB with the single

web, while Figures 6 c) and d) show both analysed supports for CWB with the double web.

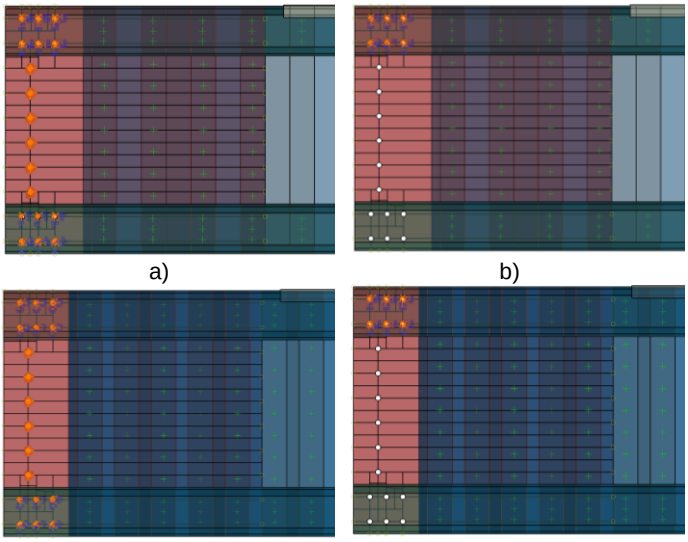

a) b) c) d)

Figure 6: End supports: a) CWB fixed, b) CWB nominally pinned, c) double CWB fixed and d) double CWB nominally pinned

The results of the analyses are presented in Figures 7 and 8.

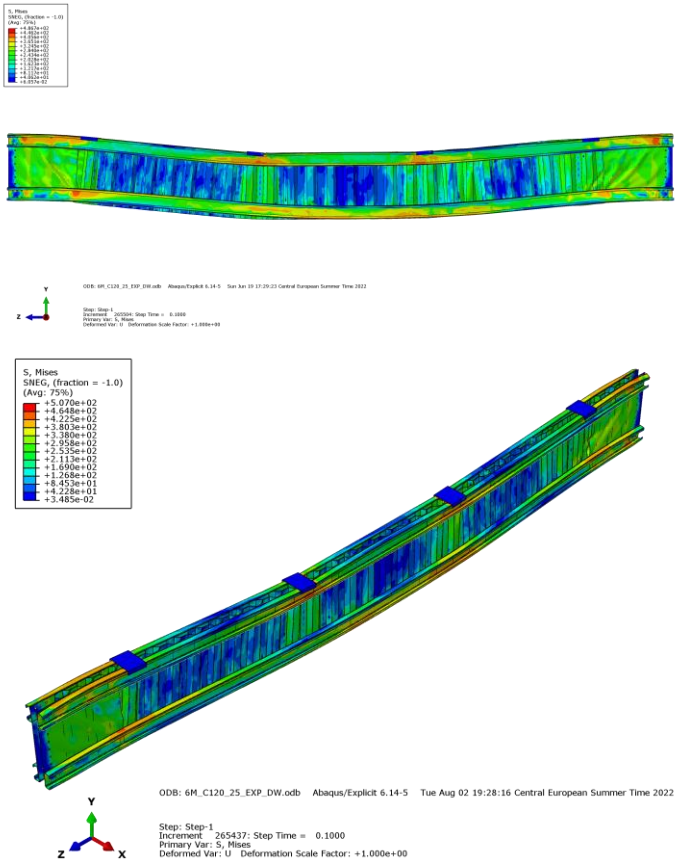

a) 6_M_C120_25_DW

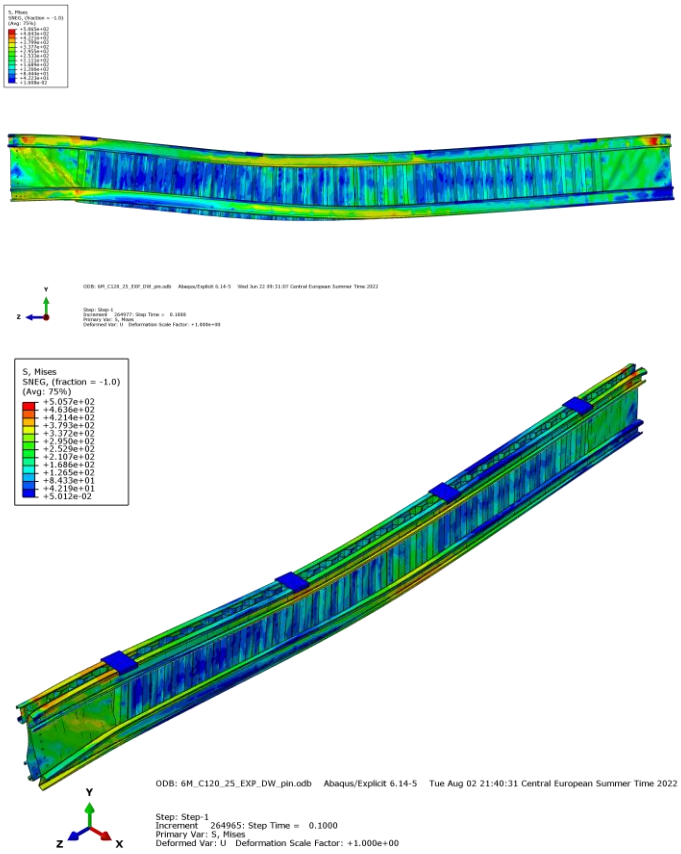

b) 6_M_C120_25_DW_pin

Figure 7: Deformed models of beams with Von Misses stress field

In Figure 8, it can be observed that double CWB results in a significantly higher bending resistance and flexural stiffness.

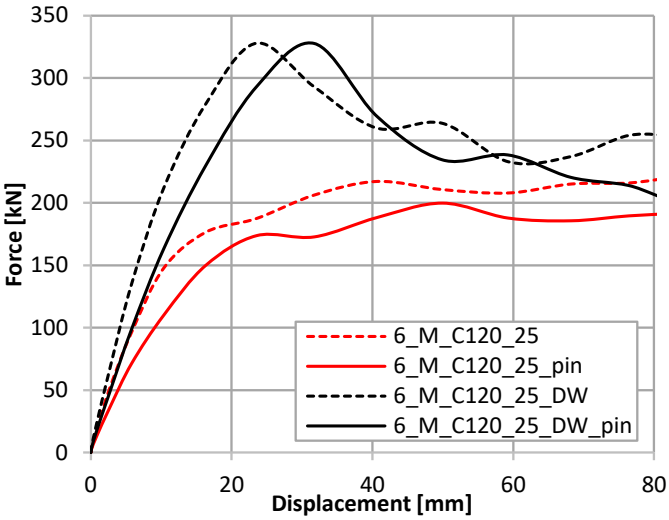

Figure 8: Influence of changing end supports from fixed to nominally pinned for CWB and double CWB

On the other hand, changing the end support conditions does not have such an impact. A certain decrease in flexural

stiffness can be observed with a neglectable decrease in bending resistance only for CWB. In contrast, resistance for double CWB remains the same for both analysed end support conditions.

As results from this study related to end supports and the number of CWs show that double CWB is superior over CWB, and nominally pinned end support shows similar behaviour as fixed in the following parametric studies, only double CWB with nominally pinned end supports are analysed.

3.2 Influence of the number of spot welds on flanges

The influence of the number of SW on the flanges has been investigated by changing the number of SW from 2 to 3 SW between the CW and C profiles, as presented in Figure 9.

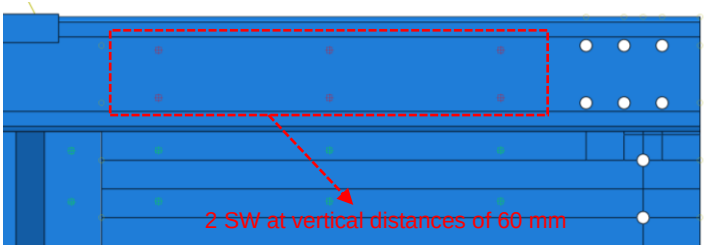

a)

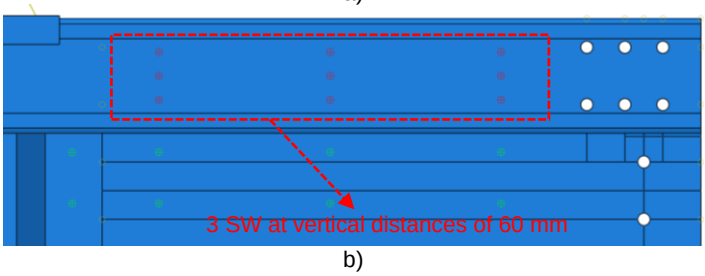

b)

Figure 9: Number of SW: a) 2SW, b) 3SW

In addition, the influence of changing from discrete to continuous TIE connections between beam elements is also investigated within this subchapter.

The results of the distance between the spot welds on the flanges and the change from discrete to continuous connections are shown in Figure 10. The model with continuous connection between beam elements shows the highest capacity and highest ductility, as expected, but such a connection is not always possible. This is why discrete connections between beam elements are investigated in more detail.

A certain influence of 3SW compared to 2SW on ultimate bending capacity can be observed, while initial flexural stiffness remains almost the same.

In the case with 3SW, the SWs were not damaged, while in the case with 2SW, the failure of the SW results in a sudden drop in flexural stiffness and bending resistance.

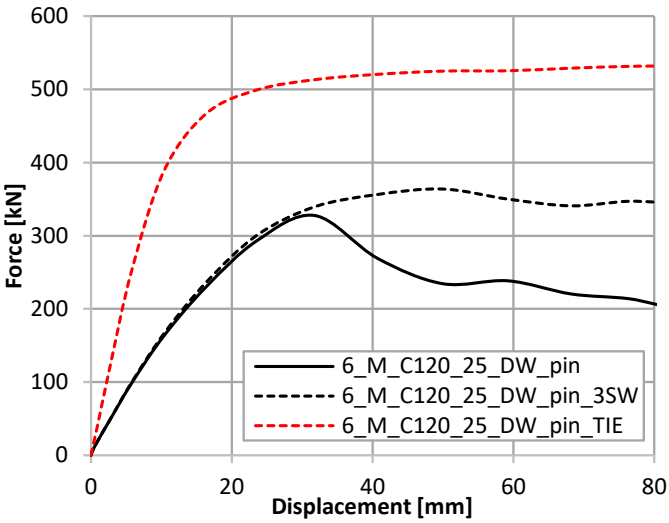

Figure 10: Influence of the number and distance between spot welds on flanges

Figure 11 shows the influence of changing discrete SW connections to continuous TIE connections and the influence of an increased number of SWs.

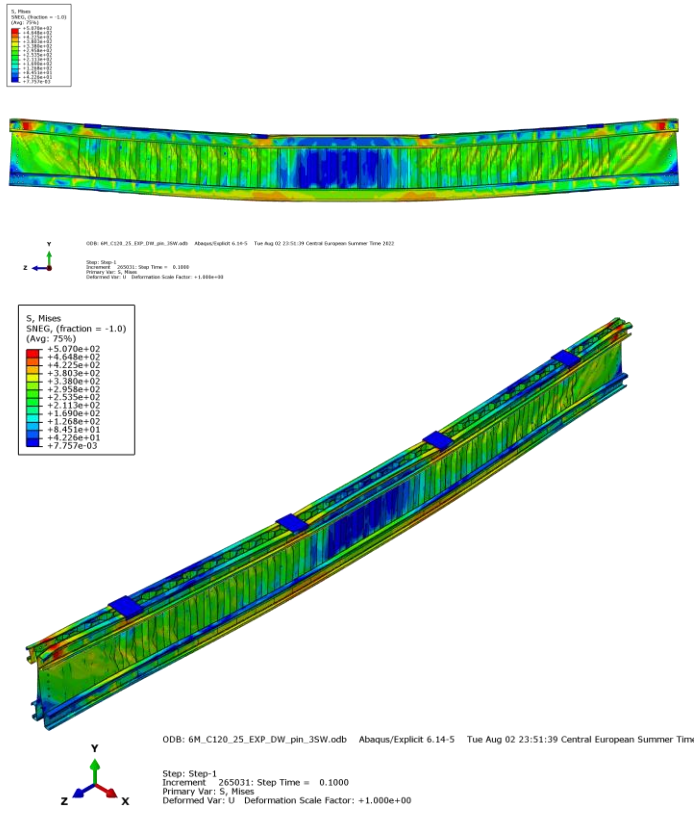

a) 6_M_C120_25_DW_pin_3SW

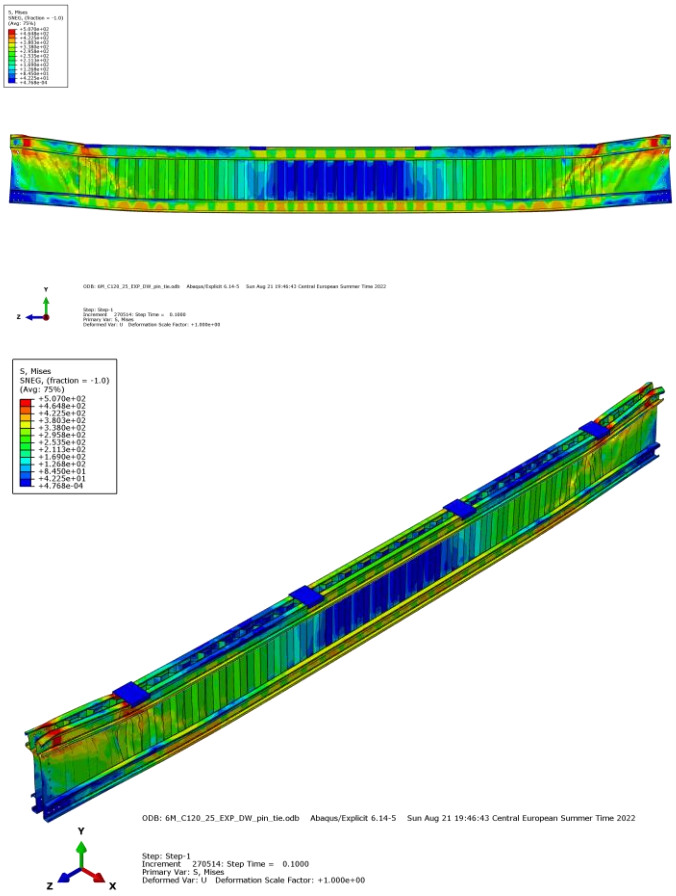

b) 6_M_C120_25_DW_pin_TIE

Figure 11: Deformed models of beams with Von Misses stress field

By comparing Figure 11 with Figure 7, it can be observed that in the cases of continuous connection between beam elements and an increase in the number of SW separation between beam elements is significantly reduced. This means that a solution with an increased number of SWs changes the beam's failure mode.

From these results, we can conclude that the number of SW can change beam capacity.

3.3 Influence of the distance between spot welds on flanges

The influence of the distance between the spot welds on the flanges has been investigated by changing the distance between SW according to Figure 12.

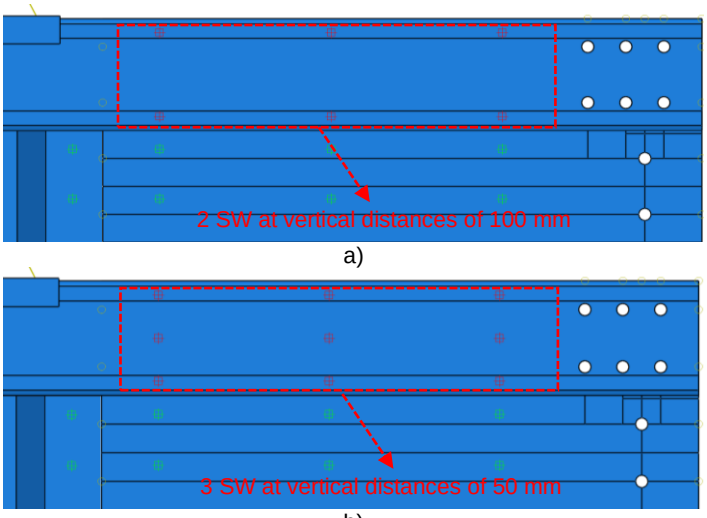

Figure 12: Increased vertical distance between SW: a) 2SW, b) 3SW

The results of the influence of the distance between the spot welds on the flanges presented in Figure 13 show a minimal influence of the increased distance between SW for 2SW. The same negligible influence can be found by comparing the results for 3SW in Figure 10 and the results for the increase in distance for 3SW in Figure 13.

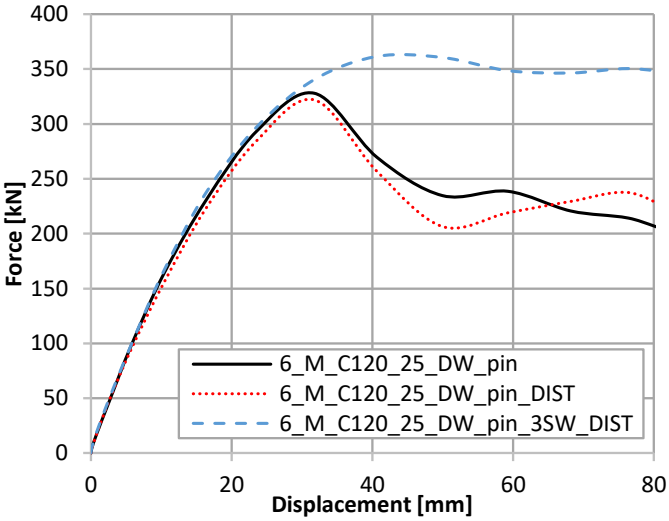

Figure 13: Influence of the distance between spot welds on flanges

3.4 Influence of the flange's thickness

The analysed thicknesses of the flanges in this study are 1.0 mm, 1.2 mm, 1.5 mm, 2.0 mm, and 2.5 mm and the results are presented in Figure 14. All models are created with 2 SW at the initial vertical distance between SW of 60 mm.

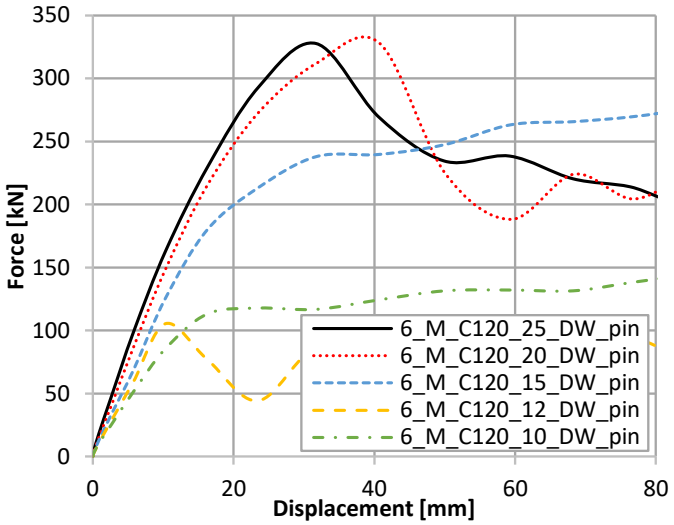

Figure 14: Influence of the flange's thickness

The results show that C profile thicknesses below 1.5 mm result in a very low beam capacity. This result is a consequence of the early instability of the flange profile, but also from the early failure of SW. The 2.0 mm and 2.5 mm thicknesses result in almost identical bending resistance with a slight increase in flexural stiffness in the case of 2.5 mm. Such behaviour is related to the similar capacity of SW for these thicknesses.

3.5 Influence of corrugated web thickness

The influence of corrugated web thicknesses has been investigated based on the model with all elements like in the model 6_M_C120_25_DW_pin, but varying the thickness of web elements only, i.e. 0.8 mm, 1.0 mm, 1.2 mm and 1.5 mm.

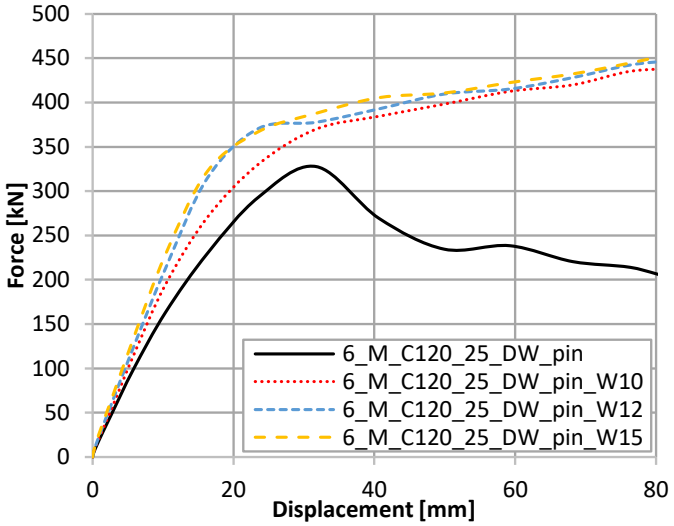

Figure 15: Influence of corrugated web thickness

Consequently, the thicknesses of the flanges and shear plates were the same for all models investigated. The results are shown in Figure 15.

Certain influences can be seen to increase the flexural stiffness and the bending capacity. In addition, similar behaviour as previously identified with an increased number of SWs has been observed. The failure mode has been changed for all models with increased corrugated web thickness, and the SWs are not failed.

3.6 Influence of the shear panel thickness

As presented in the previous cases, the thicknesses of all elements have been maintained like in the model 6_M_C120_25_DW_pin, the only variable being the thickness of shear plates, i.e. 0 mm (without SP), 0.8 mm, 1.0 mm, 1.2 mm and 1.5 mm. The results are shown in Figure 16.

The influence of the shear panel thickness is not negligible but is smaller than in the case of the web thickness from the previous case. SPs thicknesses are not connected with the change of double CWB failure mode, and for all analysed models, SW failed.

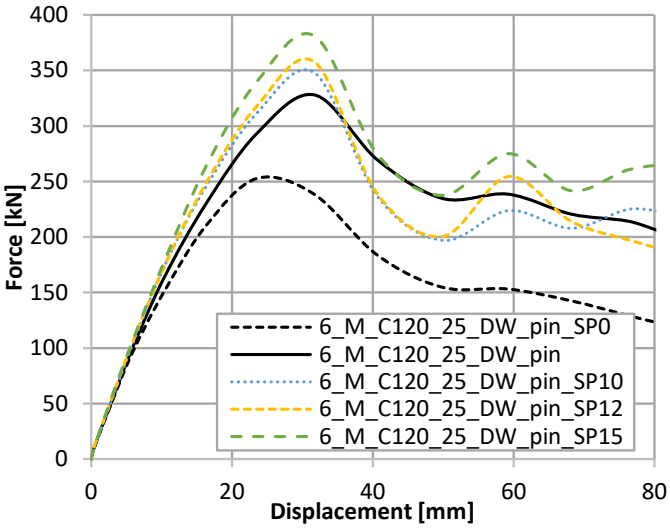

Figure 16: Influence of the shear panel thickness

3.7 Influence of increased web and shear panel thicknesses

To investigate the influence of the model with increased web and shear plate thicknesses, the web thickness and shear plate thickness were varied together, that is, 0.8 mm, 1.0 mm, 1.2 mm and 1.5 mm. The results are shown in Figure 17.

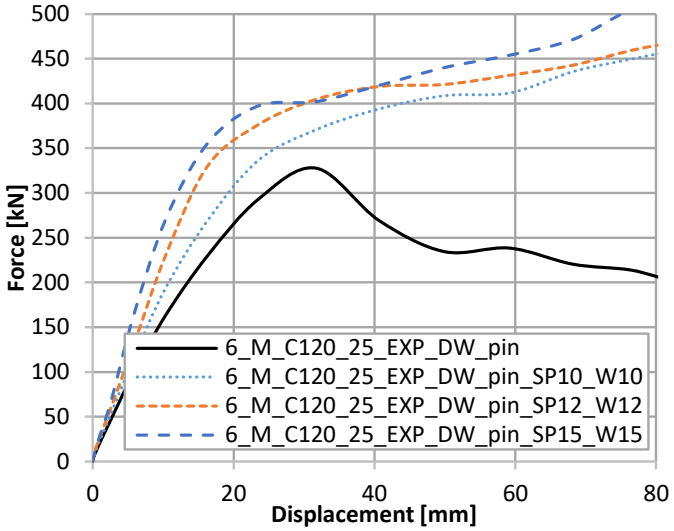

Figure 17: Influence of increased web and shear panel thicknesses

It can be concluded that increased web and shear panel thicknesses can significantly increase double CWB flexural stiffens and bending capacity.

4. Conclusions

Previously obtained experimental and numerical results on built-up cold-formed steel beams showed that such a system represents a sustainable solution in structural engineering due to material savings and ease of manipulation, but also due to the high protection against corrosion, with all components galvanised. The number of parameters governs the resistance of built-up cold-formed steel elements due to the multiple parts involved and the significant number of possible beam configurations.

- The parametric study presented shows that changing end support conditions can significantly reduce the complexity of CWB beam support and, consequently, its cost without a significant decrease in beam performance related to its rigidity and bending capacity.
- A new solution of CWB with double corrugated web significantly contributes to the rigidity and capacity of CWB.
- Changing the type of connection between beam elements from discrete SW to continuous TIE connection results in the beam's highest capacity and rigidity. On the other hand, changing the number of SW from 2 to 3 can have a certain influence on increasing the ultimate bending capacity, while the initial flexural stiffness remains almost the same. It is observed that an increased number of SW can change the beam failure mode. The models with 2SW suddenly fail due to SW failure, whereas models with 3SW do not fail due to SW failure.
- The distance between the SWs on the flanges shows minimal influence on beam behaviour.
- Decreasing the C profile thicknesses can result in very low beam capacity, especially for thicknesses below 1.5 mm.
- A higher thickness of the corrugated web increases the flexural stiffness and bending capacity of the beam, with a similar behaviour as previously identified with an increase in the number of SW, when changing the beam failure mode.
- The thickness of the shear panel is not negligible, but its influence is less than that of the thickness of the web. Changing the SPs thicknesses is not connected with the change of double CWB failure mode, and for all analysed models, SW failed.
- Combining the increased thicknesses of the web and the shear panel can significantly increase the flexural stiffness and bending capacity of the beam.

The presented study is the basis for further research to find the optimal solution in terms of steel consumption and the number of SWs for larger spans.

5. Acknowledgments

This work has been supported in part by Croatian Science Foundation under the project UIP-2020-02-2964 and by a grant of the Ministry of Research, Innovation and Digitization, CCCDI - UEFISCDI, Romania, project number PN-III-P2-2.1-PTE-2021-0237, within PNCDI III.

References

[1] Ungureanu V, Both I, Burca M, Radu B, Neagu C, Dubina D. Experimental and numerical investigations on built-up cold-formed steel beams using resistance spot welding. Thin-Walled Struct 2021;161:107456. https://doi.org/10.1016/j.tws.2021.107456.

[2] Dubina D, Ungureanu V, Gîlia L. Cold-formed steel beams with corrugated web and discrete web-to-flange fasteners. Steel Constr 2013;6:74–81. https://doi.org/10.1002/stco.201310019.

[3] Ungureanu V, Both I, Burca M, Tunea D, Grosan M, Neagu C, et al. Welding technologies for built-up cold-formed steel beams: experimental investigations. Ninth Int. Conf. Adv. Steel Struct., Hong Kong, China: 2018, p. e-Proceedings.

[4] Dassault Systèmes Simulia. Abaqus CAE User's Manual (6.12). Manuals 2012:1174.

[5] Ungureanu V, Lukačević I, Both I, Burca M, Dubina D. Built-Up Cold-Formed Steel Beams with Corrugated Webs Connected by Spot Welding - Numerical Investigations. Int. Colloq. Stab. Ductility Steel Struct. (SDSS 2019), Prague: 2019, p. e-Procedings.

[6] Ungureanu V, Lukačević I, Both I, Burca M. Numerical investigation of built-up cold-formed steel beams connected by spot welding. Evol. Mertropolis, 2019 IABSE Congr. New York City, New York: 2019, p. e-Procedings.
[7] Ungureanu V, Lukačević I, Both I, Dubina D. Numerical investigations on built-up cold-formed steel beams for long spans. Ce/Papers 2021;4:2277–84. https://doi.org/10.1002/cepa.1550.
[8] European Committee for Standardization (CEN). EN 1993-1-5: Eurocode 3: Design of steel structures - Part 1-5: General rules - Plated structural elements. Brussels: 2006.